

Moxibustion alleviates chronic heart failure by regulating mitochondrial dynamics and inhibiting autophagy

RAN XIA¹, WEI WANG¹, BING GAO¹, QIANG MA¹, JING WANG², XIAOHUA DAI³ and QINGLING LI⁴

¹Graduate School, Anhui University of Chinese Medicine, Hefei, Anhui 230012; ²Key Laboratory of

Xin'an Medicine of Ministry of Education, Anhui University of Chinese Medicine, Hefei, Anhui 230038;

³Department of Cardiovascular Medicine, The First Affiliated Hospital of Anhui University of Chinese Medicine, Hefei,

Anhui 230031; ⁴School of Chinese Medicine, Anhui University of Chinese Medicine, Hefei, Anhui 230012, P.R. China

Received November 17, 2021; Accepted February 8, 2022

DOI: 10.3892/etm.2022.11286

Abstract. Moxibustion (MOX) is a traditional Chinese medicine preparation, which has been clinically used to treat cardiac diseases in recent years. The present study aimed to examine the protective effects and possible mechanisms of MOX on doxorubicin (DOX)-induced chronic heart failure (CHF) in rats. The animals were divided into five groups, including the Control (normal saline), DOX (doxorubicin 15 mg/kg), MOX (doxorubicin 15 mg/kg + moxibustion), BEN (doxorubicin 15 mg/kg + benazepril 0.86 mg/kg) and MOX + BEN (doxorubicin 15 mg/kg + moxibustion + benazepril 0.86 mg/kg) groups. After three weeks, echocardiography was performed to assess cardiac function and structure, including left ventricular internal diameter in systole, ejection fraction and fractional shortening (FS). Serum brain natriuretic peptide levels and adenosine triphosphate (ATP) levels were measured by enzyme-linked

immunosorbent assay and ATP assay. Cardiac pathology was assessed by hematoxylin and eosin and Masson's trichrome staining. Cardiac ultrastructure and the number of autophagosomes formed were visualized by transmission electron microscopy. Western blotting was performed to assess mitochondrial dynamics, autophagy proteins and mitochondrial autophagy-related pathway proteins. The expression levels of these genes were assessed by reverse transcription-quantitative PCR. The results indicated MOX could improve cardiac function, increased cardiac ATP levels and reduced myocardial fibrosis. Western blotting indicated that MOX treatment elevated the expression of optic atrophy 1 protein (OPA1), while decreasing the expression of dynamin-related protein 1 and mitochondrial fission 1 protein. In addition, MOX inhibited autophagy, as evidenced by decreased number of autophagosomes, reduced LC3II/LC3I ratio and increased p62 expression. Furthermore, MOX downregulated DOX-induced FUNDC1 signaling pathway. In summary, MOX has protective effects on DOX-induced CHF in rats, promoting mitochondrial fusion while inhibiting mitochondrial fission and mitophagy. The underlying mechanisms may be related to the inhibition of the FUNDC1 signaling pathway.

Correspondence to: Professor Jing Wang, Key Laboratory of Xin'an Medicine of Ministry of Education, Anhui University of Chinese Medicine, 103 Meishan Road, Hefei, Anhui 230038, P.R. China

E-mail: wangjing2161@126.com

Professor Xiaohua Dai, Department of Cardiovascular Medicine, The First Affiliated Hospital of Anhui University of Chinese Medicine, 117 Meishan Road, Hefei, Anhui 230031, P.R. China

E-mail: xin_d3980@163.com

Abbreviations: BEN, benazepril; BNP, serum brain natriuretic peptide; CHF, chronic heart failure; DOX, doxorubicin; DRP1, dynamin-related protein 1; EF, ejection fraction; FIS1, fission 1 protein; FS, fractional shortening; FUNDC1, FUN14 domain-containing protein 1; H&E, hematoxylin and eosin; MOX, moxibustion; mRNA, messenger RNA; OPA1, optic atrophy 1; PGAM5, phosphoglycerate mutase family member 5; RT-qPCR, reverse transcription-quantitative PCR; ULK1, Unc-51 Like Autophagy Activating Kinase 1

Key words: moxibustion, chronic heart failure, mitochondrial fission, mitochondrial fusion, mitophagy, pathway

Introduction

Chronic heart failure (CHF), a major public health concern worldwide, is a complex clinical syndrome, in which the heart cannot pump enough blood to meet the body's requirements, resulting in a series of clinical symptoms, including dyspnea, weakness and lower limb swelling (1). The ASIAN-HF study reported that the onset of heart failure (HF) is closely related to hypertension, anemia, diabetes, coronary artery disease (CAD), atrial fibrillation and obesity, contributing to a high morbidity (2). In China, the overall prevalence of HF has increased by 44% during the past 15 years in patients aged >35 years (3). Despite great advances in the treatment of CHF (4), further research is required to alleviate its symptoms and decrease the morbidity, mortality and re-hospitalization rates in CHF patients (5). Therefore, the development of novel therapeutic approaches targeting CHF-associated pathways is of great significance, to treat CHF more effectively.

CHF is a progressive disease, in which long-term ischemia and hypoxia may lead to myocardial cell necrosis and ventricular remodeling (6,7). Therefore, effective protection of cardiomyocytes can decelerate the progression of CHF (8). Mitochondria may not only synthesize a large amount of adenosine triphosphate (ATP) for myocardial cells, but also participate in metabolism, signaling, redox balance and ion homeostasis (9,10). Damaged mitochondria produce reactive oxygen species (ROS), leading to oxidative stress and cardiomyocyte death (11). The homeostasis of myocardial mitochondria depends on mitochondrial dynamics and autophagy. FUN14 domain-containing protein 1 (FUNDC1) is an integral mitochondrial outer-membrane protein, which mediates the formation of mitochondria-associated endoplasmic reticulum membranes (12). In humans, mitochondrial fusion is mediated by the dynamin-related GTPases mitofusin 1 and mitofusin 2 (MFN1 and MFN2) and optic atrophy 1 (OPA1), which mediate outer mitochondrial membrane (OMM) and inter mitochondrial membrane (IMM) fusion, respectively (13). However, under myocardial ischemic and hypoxic conditions, FUNDC1 interacts with dynamin-related protein 1 (DRP1), mitochondrial fission 1 protein (FIS1) and LC3 to induce excessive mitochondrial fission and autophagy, leading to cell death (14,15). In addition, de-phosphorylation of phosphoglycerate mutase family member 5 (PGAM5) and phosphorylation of Unc-51 Like Autophagy Activating Kinase 1 (ULK1) may activate FUNDC1 to interact with LC3 for autophagosome recruitment (16,17). Therefore, FUNDC1 plays an important role in myocardial mitochondrial dynamics and autophagy.

Moxibustion (MOX), an important component of traditional Chinese medicine (TCM), has been widely and effectively used in the treatment of chronic diseases. Previous studies have shown that MOX possesses therapeutic effects in coronary heart disease (18,19). Our research group previously explored its protective effects on the heart and demonstrated that MOX can downregulate inflammatory factors while upregulating anti-inflammatory factors (20). MOX can regulate autophagy by inducing the activation of the mechanistic target of rapamycin (mTOR) signaling pathway (21,22). Hence, the present study aimed to investigate whether MOX could mediate mitochondrial dynamics and autophagy to alleviate CHF in a doxorubicin (DOX)-induced animal model.

Materials and methods

Laboratory animals. A total of 100 male Sprague-Dawley rats (aged, 8 weeks; body weight, 200-250 g) were obtained from the Anhui University of Chinese Medicine [Hefei, China; animal license number: SCXK (Shandong) 2019-003]. They were housed in accordance with animal welfare regulations, under specific-pathogen-free conditions at 25°C, humidity of 50% and a 12-h light/dark cycle. The rats had free access to food and water and were fasted 12 h before the operation. All animal experiments were approved by the Ethics Committee of the Anhui University of Chinese Medicine (approval no. AHUCM-rats-2020026). The present study followed the Guide for the Care and Use of Laboratory Animals of the National Institutes of Health (23).

Animal group and CHF modeling. The 100 rats were assigned into Control group (C, n=20), Doxorubicin group (DOX, n=20), Moxibustion group (MOX, n=20), Benazepril (BEN, n=20) and Moxibustion + Benazepril group (MOX + BEN, n=20), using a random number table.

The rats in the Control group were fed normally. CHF models were established according to the method reported by Leontyev *et al.* (24) in all groups except the control group. Doxorubicin injection solution (1 mg/ml) was prepared in 0.9% saline and 80 rats were injected with doxorubicin at 2.5 mg/kg intraperitoneally once a week for 6 consecutive weeks, with a cumulative injection volume of 15 mg/kg. Following the last injection, the successful model construction was judged by echocardiography. After one week of adaptive feeding, the intervention treatment was started after the 7th week.

Rats in the C group and DOX group were given the equal dose of normal saline once a day for three consecutive weeks. Rats in the MOX group were placed on a platform and underwent moxibustion at Feishu (BL13, 7 mm below the third thoracic spinous process on both sides) and Xinshu (BL15, 7 mm below the fifth thoracic spinous process bilaterally) points using moxibustion sticks (5x120 mm; Wolong Traditional Chinese Medicine Moxibustion Factory) to make the temperature of the acupuncture points up to 44±1°C (25), once a day for three consecutive weeks. Rats in the BEN group were administered with 0.86 mg/kg benazepril (Novartis International AG) by gavage once per day for 3 consecutive weeks (26). Rats in the MOX + BEN group received combined treatment with moxibustion and benazepril (0.86 mg/kg) once a day for three consecutive weeks. The study flowchart is shown in Fig. 1.

During the experimental period, the general condition of the rats, including diet, coat color, mental status, activity and respiratory function of rats were observed every day and body weight were measured every 2 days. When rats exhibited extreme weakness, anorexia, weight loss (≥20%), multiple skin sores that would not heal, respiratory disorders, cyanosis and continuous poor sense of balance, sacrifice by overdose of anesthesia (150 mg/kg sodium pentobarbital intraperitoneal injection) was immediately performed. There were no deaths in the C group. A total of seven rats died in the DOX group, four rats died in the MOX group, three rats died in the BEN group and two rats died in the MOX + BEN group. Specifically, nine rats reached the humane endpoints by showing clear anorexia and depression, weight loss (≥20%) and extreme weakness. Three rats had to be sacrificed as they developed dyspnea and were unable to stand. Two rats were immediately sacrificed with severe infection and non-healing ulcers on the abdomen. Two rats were found dead when fed early morning. It was speculated that the death may have been caused by fatal arrhythmias. Of the 100 rats, 84 rats completed the study and the lethal rate of doxorubicin was 20% throughout the experiment (24).

At the end of the experiment, surviving experimental rats were intraperitoneally injected with 3% sodium pentobarbital at a dose of 30 mg/kg and blood was collected from the abdominal aorta. Then rats were euthanized (cervical dislocation) and the heart tissue was removed after the rat's vital signs disappeared.

Echocardiographic assessment. Intraperitoneal injection of 3% pentobarbital sodium was performed for anesthesia at a dose of 30 mg/kg and left ventricular cardiac function was

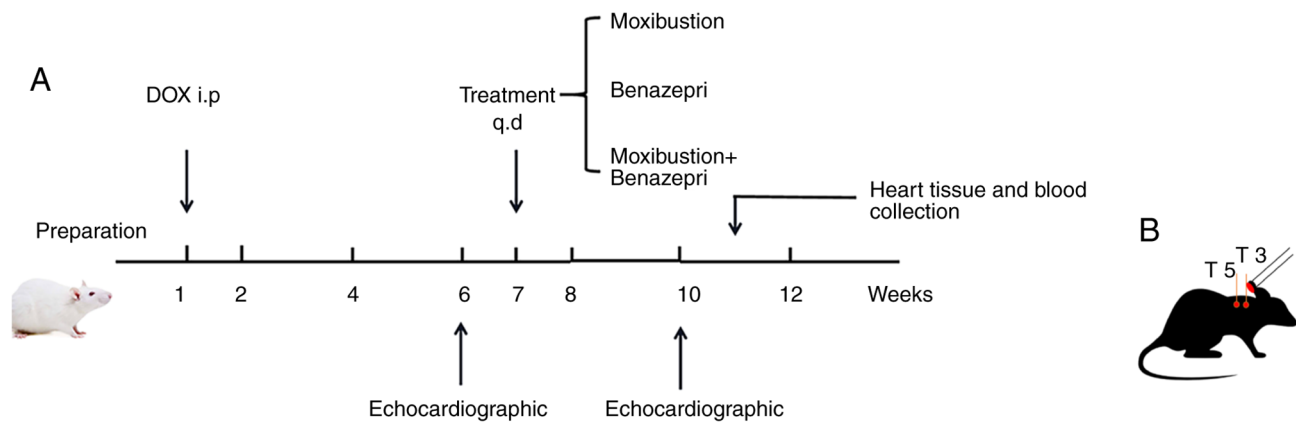


Figure 1. The study design of the experiment. (A) The study flowchart. (B) Diagram of moxibustion in rats. A moxa stick of 5 mm in diameter was ignited and placed 2-3 cm above the bilateral Feishu (T3) and Xinshu (T5) for 20 min per day. i.p.: intraperitoneal injection; qd, quaque die; DOX, doxorubicin.

assessed by echocardiography in the two-dimensional B-mode and M-mode (Siemens Acuson Oxana 3; Siemens AG), with left ventricular internal diameter in systole (LVIDS), ejection fraction (EF) and fractional shortening (FS) tested for at least three nonstop cardiac cycles. Transthoracic echocardiography was performed immediately at 6 (to assess molding success) and 10 (to assess treatment effect) weeks.

Pathological staining. Myocardial tissue samples were fixed with 4% paraformaldehyde for 72 h at 4°C and dehydrated using alcohol gradient (70, 80, 90 and 100%) alcohol at room temperature. The sections were infiltrated in paraffin for 30 min at 65°C and embedded in paraffin wax. The sections were cut into 5- μ m slices using a Leica Biosystems RM2245 microtome (Leica Microsystems GmbH). After dewaxing with dimethyl benzene and rehydration with descending alcohol series. Paraffin-embedded tissue sections were stained with hematoxylin and eosin (H&E) and Masson's trichrome to assess histopathological features and cardiac fibrosis, respectively.

For the H&E staining, sections were stained with hematoxylin at room temperature for 5 min, 1% HCl-alcohol differentiation for 5-30 sec, staining with an eosin staining solution for 5 min at room temperature. The sections were dehydrated with 95% alcohol for 5 min at room temperature then were cleared with xylene for 5 min and finally sealed with neutral balsam. The tissue sections were subsequently visualized under a light microscope at a magnification of x400 (Leica Microsystems GmbH).

For Masson's trichrome staining, the sections were stained with Wiegert iron hematoxylin solution (cat. no. G1340; Beijing Solarbio Science and Technology Co., Ltd.) for 5 min at room temperature, then were treated with Ponceau fuchsin acid solution for 5-10 min. After washing in distilled water, the sections were treated with 1% aqueous solution of phosphomolybdic acid for 1-3 min. Without washing with water, the sections were treated with aniline blue for 3-6 min. Finally, the sections were treated with 1% glacial acetic acid for 1 min, dehydrated with ethanol and were cleared with xylene for 5 min and sealed with neutral balsam. Light microscopy was subsequently conducted at a magnification of x400 (Nikon Corporation). The severity of myocardial fibrosis was analyzed from tissue sections stained with Masson's trichrome with the Image-Pro Plus 6.0 software (Media Cybernetics Inc.).

Enzyme-linked immunosorbent assay (ELISA). Blood samples (1.5 ml) were collected from the abdominal aorta, centrifuged at 1,500 x g at 4°C for 15 min and examined with an ELISA kit according to the manufacturer's instructions (cat. no. E-EL-R0126c; Wuhan Elabscience Bio-Tech Co., Ltd.) to detect serum BNP levels.

Measurement of ATP content. Fresh myocardial tissue samples were obtained from the left ventricle and 20 mg was added to 100 μ l lysis buffer, followed by thorough homogenization. After centrifugation at 11,290 x g at 4°C for 5 min, the supernatant was collected. ATP was detected with a specific kit (cat. no. S0026; Beyotime Biotechnology) as directed by the manufacturer. Relative light intensity (RLU) was assessed on a plate reader.

Transmission electron microscopy (TEM). Fresh myocardial tissue samples (1 mm³) were fixed with 2% glutaraldehyde at 4°C for at least 2 h, washed with PBS 3 times (10 min each). This was followed by another fixation with 1% osmium tetroxide at 20°C for 2 h and 3 washes with PBS. The tissue samples were dehydrated with graded ethanol (50, 70, 80 and 90%) for 15 min each and dehydrated with 100% acetate 3 times for 20 min each at room temperature. The tissue samples were embedded using epoxy resin at room temperature overnight and sliced into ultrathin sections (60-70 nm) with an ultramicrotome. The ultrathin sections were stained with 2% uranium acetate saturated alcohol solution and lead citrate 15 min each at room temperature. Stained sections were visualized using HT7800 transmission electron microscope (magnification x2,500 and x7,000) and autophagosomes were counted with the Gatan Digital Micrograph software (v 3.5; Gatan, Inc.).

Western blotting. Myocardial tissue samples were obtained from the left ventricle and proteins were extracted with chilled radio-immunoprecipitation assay (RIPA) buffer (Beyotime Institute of Biotechnology). Following homogenization, the tissue was lysed and centrifuged at 11,290 x g at 4°C for 10 min and the resulting supernatant was collected. Total protein levels were determined with a BCA kit (Beijing Solarbio Science & Technology Co., Ltd.). To detect the expression levels of FUNDC1, phosphorylated (p-) FUNDC1, PGAM5, ULK1, OPA1, DRP1, FIS1, LC3I, LC3II and p62

in cardiac tissue specimens, 50 μ g of proteins were resolved by sodium dodecyl sulfate-polyacrylamide gel electrophoresis (SDS-PAGE), followed by transfer onto polyvinylidene fluoride (PVDF) membranes. The membranes were incubated with anti-FUNDC1 (1:2,000; cat. no. 49240; CST Biological Reagents Co., Ltd.), anti-p-FUNDC1 (1:2,000; cat. no. AF0001; Affinity Biosciences), anti-PGAM5 (1:2,000; cat. no. ab244218; Abcam), anti-ULK1 (1:5,000; cat. no. 8054; Abcam), anti-OPA1 (1:2,000; cat. no. ab157457; Abcam), anti-DRP1 (1:2,000; cat. no. ab184247; Abcam), anti-FIS1 (1:2,000; cat. no. ab156865; Abcam), anti-LC3 II (1:2,000; cat. no. 43566; CST Biological Reagents Co., Ltd.), anti-LC3 I (1:2,000; cat. no. 12741; CST Biological Reagents Co., Ltd.), anti-P62 (1:2,000; cat. no. ab109012; Abcam) and anti-glyceraldehyde 3-phosphate dehydrogenase (GAPDH; 1:2,000; cat. no. K106389P; Beijing Solarbio Science & Technology Co., Ltd.) primary antibodies for 1 h at room temperature in a dark room. Then, the membranes were incubated with horseradish peroxidase (HRP)-conjugated secondary antibodies (1:3,000; cat. no. SE134; Beijing Solarbio Science & Technology Co., Ltd.) at room temperature for 1-2 h and exposed to an ECL Substrate kit (Beijing Solarbio Science & Technology Co., Ltd.). The protein levels were normalized to those of β -actin and semi-quantification was performed with the ImageJ 1.8 software (National Institutes of Health).

Reverse transcription-quantitative (RT-q) PCR. ULK1, PGAM5 and FUNDC1 mRNA levels in heart tissue samples were detected by RT-qPCR. According to the manufacturer's protocol, total RNA from each sample was extracted with Trizol reagent (cat. no. B511321; Shanghai Sangon Biotech Co., Ltd.). The EasyScript One-Step gDNA Removal and cDNA Synthesis SuperMix kit (cat. no. AE311-02; Beijing Transgen Biotech Co., Ltd.) was used for reversing transcriptase at the conditions of 42°C for 15 min and cRNA was synthesized. A TransStart Green qPCR SuperMix kit (cat. no. AQ131-01; Beijing Transgen Biotech Co., Ltd.) was used to perform qPCR. The reaction volume was 20 μ l (2X Top Green EX-Taq Mix 10 μ l, QF 0.5 μ l, QR 0.5 μ l, Template cDNA 2 μ l, RNase free dH₂O 7 μ l). The subsequent PCR amplification was carried out for 2 min at 95°C, followed by 40 cycles of 15 sec at 95°C, 20 sec at 57°C and 30 sec at 72°C, with final extension at 95°C for 15 sec. Each reaction was repeated in triplicate. The relative expression levels were calculated by the 2^{- $\Delta\Delta$ C_q} method and GAPDH was used as an internal control (27). The primers used for RT-qPCR are shown in Table I.

Statistical analysis. The data were statistically analyzed with the SPSS 24.0 software (IBM Corp.) and expressed as mean \pm standard deviation (SD). Comparisons in multiple groups were performed by one-way analysis of variance (ANOVA) and Dunnett's test was utilized for group pair comparisons. P<0.05 was considered to indicate a statistically significant difference.

Results

Effects of MOX on cardiac function and morphological alterations of the myocardium in the rat model of CHF. After 10 weeks, echocardiography revealed reduced EF and FS in the DOX group compared with the C group (P<0.01, Fig. 2). LVIDS values were elevated in the DOX group (P<0.01,

Table I. The sequences of primers used for reverse transcription-quantitative PCR.

Gene	Primers (5'→3')
ULK1	GGCTCTATTGCAGCGTAACC GCACAGGTGGGGATTTCTTGA
PGAM5	AGACTTGCTACGGGAAGGTG GCATCAGCTCGGTGGATGTA
FUNDC1	TGTGATATCCAGCGGCTTCG TGCTGCCACAGTCTTCCTCT
GAPDH	GGAAAGCTGTGGCGTGAT TCCACAACGGATACATTGGG

ULK1, Unc-51 Like Autophagy Activating Kinase 1; PGAM5, phosphoglycerate mutase family member 5; FUNDC1, FUN14 domain-containing protein 1.

Fig. 2B), indicating alterations in cardiac structure and function. Serum BNP levels were significantly elevated in the DOX group compared with the C group (P<0.01, Fig. 2E). After 3 weeks of treatment, compared with the DOX group, EF and FS were significantly increased in the MOX group, whereas serum BNP levels were significantly decreased (EF and FS, P<0.01; BNP, P<0.05; Fig. 2C-E). BEN and MOX had similar effects and MOX + BEN exerted more pronounced effects compared with each single therapy (Fig. 2).

MOX ameliorates myocardial dysfunction and fibrosis. H&E staining showed that cardiomyocytes in the left ventricle were arranged in an orderly manner in the C group, but loosely arranged in the DOX group. After 3 weeks of treatment, these pathological changes were reversed in the MOX, BEN and MOX + BEN groups compared with the C group (Fig. 3A). Masson's trichrome staining showed a greater severity of cardiac fibrosis in the DOX group than in the C group (P<0.01, Fig. 3B). After 3 weeks of treatment, compared with the DOX group, collagen volume fractions were decreased in the MOX, BEN and MOX + BEN groups (Fig. 3C). In addition, MOX + BEN was more effective in improving vacuolar degeneration of cardiomyocytes and myocardial fibrosis.

Moxibustion improves myocardial ATP content. ATP levels were significantly reduced in the DOX group compared with the C group (P<0.01, Fig. 3D). After 3 weeks of treatment, compared with the DOX group, ATP levels in the MOX group were significantly increased (P<0.01, Fig. 3D). BEN and MOX had similar effects and MOX + BEN had more pronounced effects compared with each single therapy (Fig. 3D).

Effects of MOX on mitochondrial dynamics in the rat model of CHF. Western blotting showed that OPA1 expression levels were significantly decreased in the DOX group compared with the C group (P<0.01, Fig. 4), while DRP1 and FIS1 levels were significantly increased (P<0.01, Fig. 4). These results indicated reduced mitochondrial fusion and induced fission in the rat

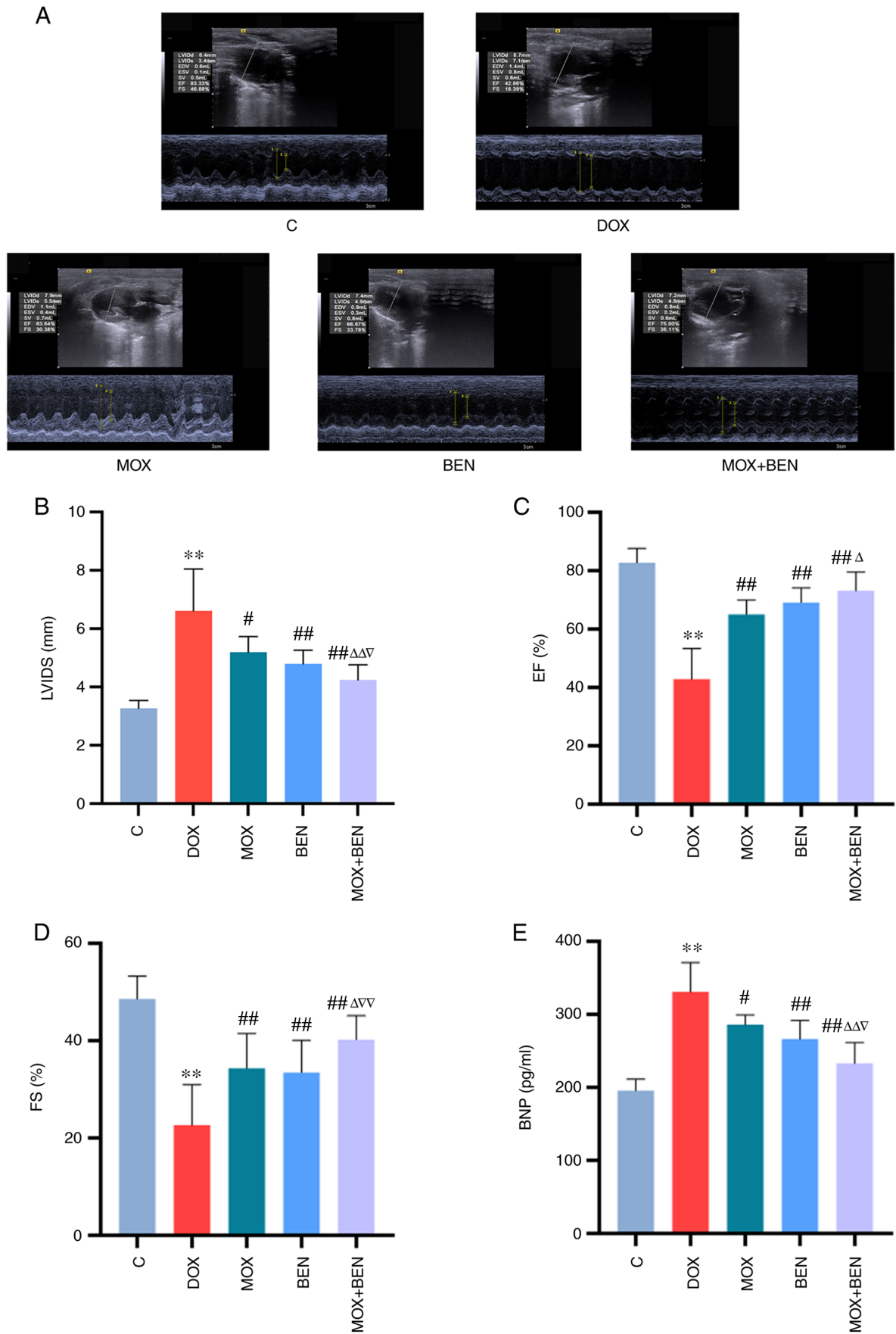


Figure 2. Effects of MOX on DOX-induced CHF in rats. (A) Representative M-mode echocardiograms. (B) LVIDS. (C) EF. (D) FS. (E) BNP. **P<0.01 vs. C group. #P<0.05 vs. DOX group. ##P<0.01 vs. DOX group. ^ΔP<0.05 vs. MOX group. ^{ΔΔ}P<0.01 vs. MOX group. [∇]P<0.05 vs. BEN group. ^{∇∇}P<0.01 vs. BEN group. Data are mean ± standard deviation from five independent experiments (n=13-20). MOX moxibustion; DOX, doxorubicin; CHF, chronic heart failure; LVIDS, left ventricular internal diameter in systole; EF, ejection fraction; FS, fractional shortening; BNP, serum brain natriuretic peptide; BEN, benazepril; C, control.

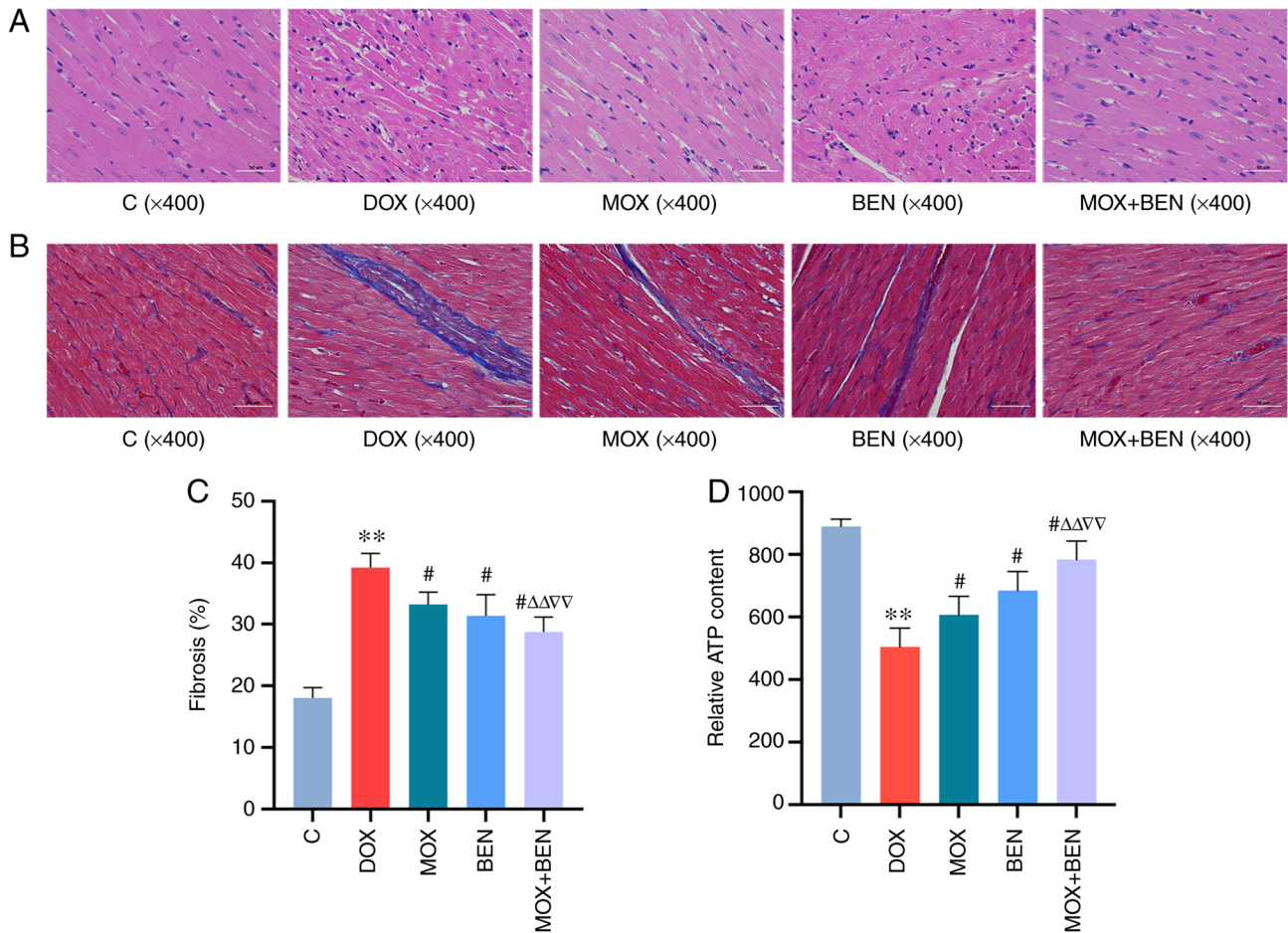


Figure 3. Effects of MOX on myocardial hypertrophy, fibrosis and cardiac mitochondrial ATP levels after DOX-induced CHF in rats. (A) Representative images of heart tissues, displaying hematoxylin and eosin staining of tissue samples from rats after 11 weeks (scale bar=50 μ m). (B) Masson's trichrome staining of tissue samples from rats after 11 weeks (scale bar=50 μ m). (C) The areas of cardiac fibrosis were quantified by Masson's trichrome staining. (D) Relative ATP levels. **P<0.01 vs. control group. #P<0.01 vs. DOX group. ΔP<0.01 vs. MOX group. ∇P<0.01 vs. BEN group. Data are mean \pm standard deviation from five independent experiments (n=13-20). MOX moxibustion; DOX, doxorubicin; CHF, chronic heart failure; BEN, benazepril; C, control.

model of CHF. Compared with the DOX group, the MOX, BEN and MOX + BEN groups showed upregulated OPA1 (P<0.01, Fig. 4) and downregulated DRP1 and FIS1 (P<0.01, Fig. 4). In addition, a greater regulation of mitochondrial dynamics was detected in the MOX + BEN group compared with the other groups (Fig. 4).

Effects of MOX on autophagy in the rat model of CHF.

Mitochondria and autophagosomes were observed by TEM. In the control group, mitochondrial structure was normal and very few autophagosomes were observed. In the DOX group, mitochondria were sparsely swollen and vacuolated, accompanied by lipid deposition and the number of autophagosomes was significantly increased. The MOX and BEN groups also had mitochondrial damage, but the number of autophagosomes was decreased compared with DOX group. The structure and arrangement of mitochondria in the MOX + BEN group were relatively normal and the number of autophagosomes was significantly reduced (Fig. 5). Western blotting revealed elevated LC3II/LC3I ratio in the DOX group compared with the C group (P<0.01, Fig. 5C and E), while p62 was markedly downregulated (P<0.01, Fig. 5C and F). Meanwhile LC3II/LC3I ratio

were reduced in the MOX, BEN and MOX + BEN groups compared with the DOX group, whereas the p62 was upregulated (Fig. 5C and E). Taken together, MOX played a protective role in DOX-induced CHF in rats by inhibiting excessive mitochondrial autophagy.

MOX inhibits the FUNDC1 pathway in the rat model of CHF.

The present study further investigated the role of the FUNDC1 pathway, which is closely correlated with mitochondrial dynamics and mitophagy (14,15). ULK1 and PGAM5, as upstream effectors of FUNDC1, could activate the FUNDC1 pathway in cardiomyocytes under hypoxic conditions or mitochondrial damage (16,17). Western blotting demonstrated that ULK1, PGAM5, FUNDC1 and p-FUNDC1 protein levels were significantly increased in the DOX group compared with the C group (P<0.01, Fig. 6) and significantly reduced in the MOX group compared with the DOX group (P<0.01, Fig. 6). Similarly, these proteins were markedly downregulated in the BEN and MOX + BEN groups. Finally, RT-qPCR revealed that ULK, PGAM5 and FUNDC1 mRNA levels were elevated in the DOX group compared with the C group (P<0.01, Fig. 6) and decreased in the MOX group compared with the DOX group (P<0.01, Fig. 6).

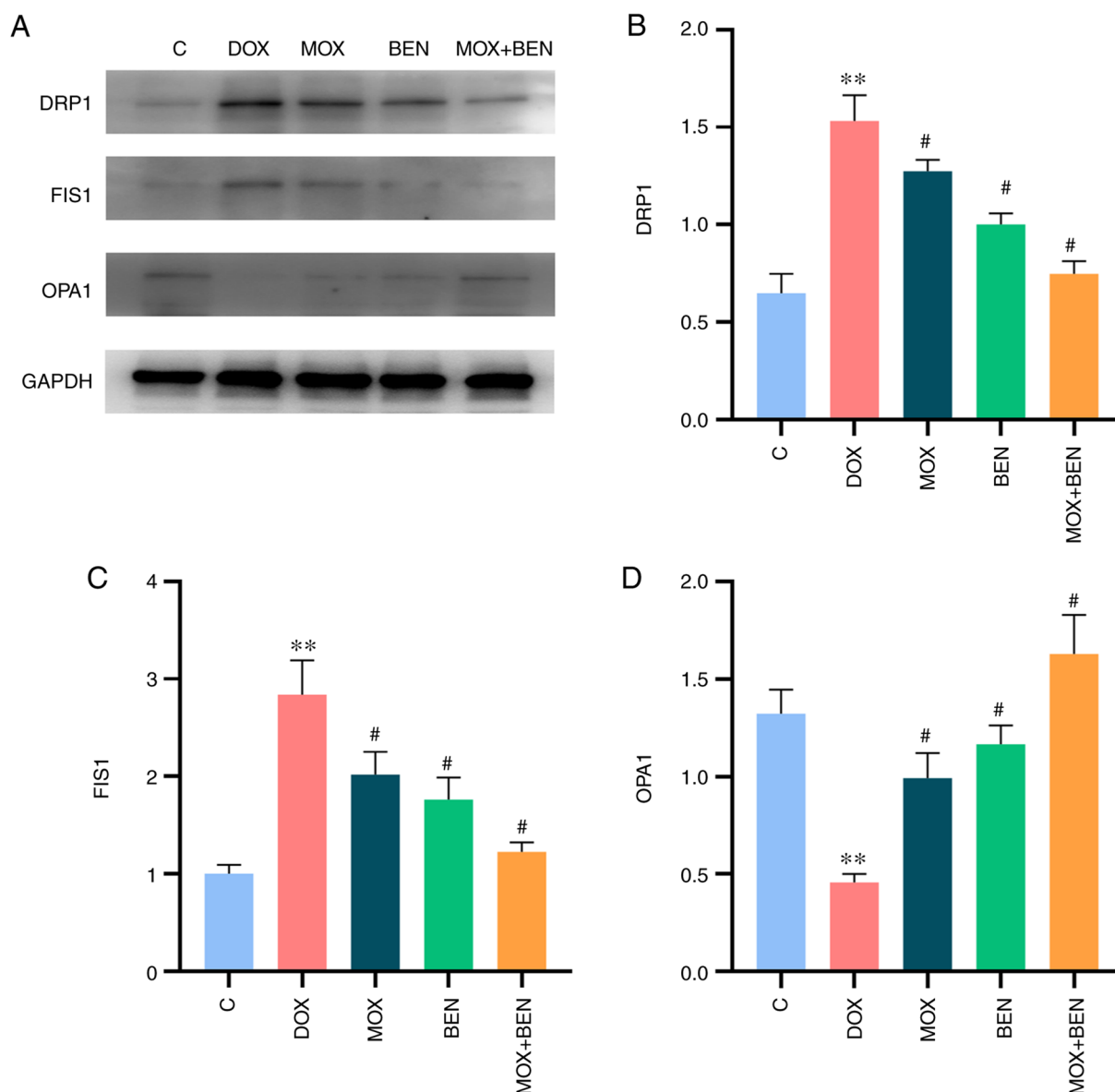


Figure 4. Effects of MOX on mitochondrial dynamics in the rat model of CHF. (A) Expression levels of DRP1, FIS1, OPA1 and GAPDH. (B) DRP1 relative to GAPDH. (C) FIS1 relative to GAPDH. (D) OPA1 relative to GAPDH. ** $P < 0.01$ vs. C group and # $P < 0.01$ vs. DOX group. Data are mean \pm standard deviation from five independent experiments (n=13-20). MOX moxibustion; CHF, chronic heart failure; DRP1, dynamin-related protein 1; FIS1, fission 1 protein; OPA1, optic atrophy 1; BEN, benazepril; C, control.

Discussion

In the present study, *in vivo* experiments were conducted to assess the protective effects of MOX in CHF and to explore the underlying molecular mechanism. The main findings could be summarized as follows: i) MOX improved the cardiac function of rats with DOX-induced CHF by regulating mitochondrial dynamics and inhibiting mitophagy; ii) The effects on mitochondrial dynamics and mitophagy could be related to the regulation of the FUNDC1 pathway; and, iii) MOX + BEN therapy showed a higher efficacy compared with the single administration of MOX or BEN.

MOX is a form of heat therapy that utilizes the burning of the herb *Artemisia Argyi* (also known as Chinese mugwort) on or around acupuncture points. This herb specifically relieves respiratory difficulty, alleviates aches and pain in joints and muscles and promotes blood circulation (28-31). As an important

component of TCM, it has been widely used in the treatment of a variety of diseases, including primary insomnia, breast cancer-related lymphedema, primary dysmenorrhea, knee osteoarthritis and inflammatory bowel disease, with significant therapeutic effects (32-37). In recent years, MOX has also been used to treat cardiovascular diseases. A pilot controlled clinical trial showed that MOX could lower blood pressure in patients with prehypertension or stage I hypertension (38). Furthermore, acupuncture and MOX have been widely applied to treat hyperlipidemia in clinical practice (39). In addition, the combination of acupuncture and MOX could improve cardiac function of patients with HF in clinical practice (40). In the present study, MOX increased the levels of indicators of cardiac function (e.g., BNP, LVIDS, EF and FS) and attenuated myocardial fibrosis.

Maintenance of mitochondrial function and integrity is imperative for the myocardium and other tissues with high energy demand (41). However, prolonged and/or high-level

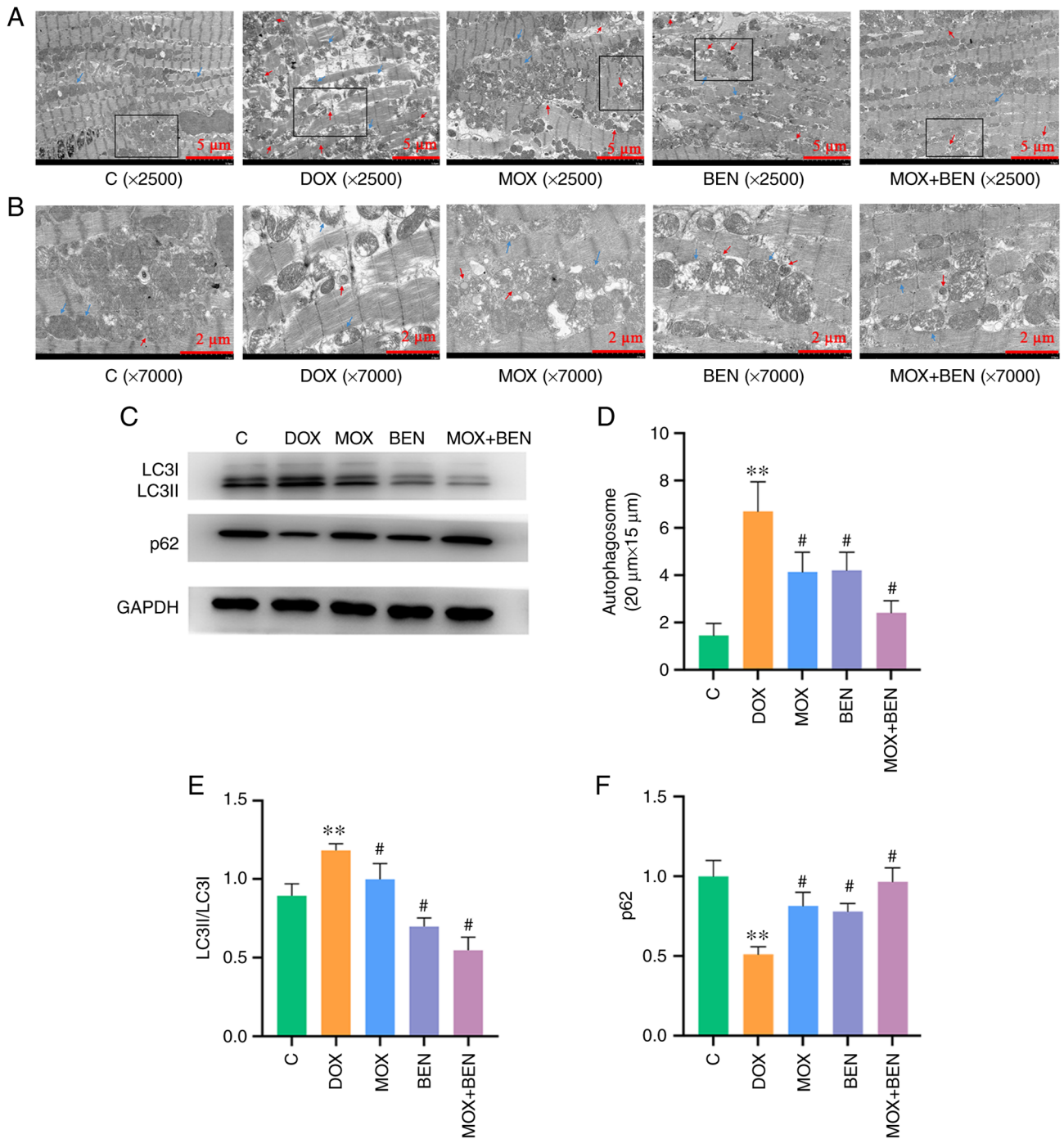


Figure 5. Effects of MOX on mitophagy in the rat model of CHF. (A) Transmission electron microscopy images. Blue arrow, mitochondria; red arrow, autophagosome. Magnification, x2,500; scale bar=5 μm. (B) Enlarged image of autophagosome structure in black frame area. Blue arrow, mitochondria; red arrow, autophagosome. Magnification, x7000; scale bar=2 μm. (C) Expression levels of LC3I, LC3II, p62 and GAPDH. (D) The number of autophagosomes in each group in the 20x15 μm area. (E) LC3II/LC3I relative to GAPDH. (F) p62 relative to GAPDH. **P<0.01 vs. C group and #P<0.01 vs. DOX group. Data are mean ± SD from five independent experiments (n=13-20). MOX moxibustion; CHF, chronic heart failure; DOX, doxorubicin; BEN, benazepril C, control.

cardiac stress causes mitochondrial damage and ATP level reduction, which are associated with HF progression and ventricular remodeling (42). The present study found that DOX decreased ATP levels in the myocardium, which were increased by moxibustion. In addition, it was observed that after moxibustion treatment, mitochondrial structure and morphology were somewhat different. These findings indicated that moxibustion improves the damaged mitochondria.

Mitochondrial dynamics and mitophagy cooperatively act to determine cardiac mitochondrial function and integrity, as well as to promote cardiomyocyte cell survival (43). OPA1, a mitochondrial fusion protein, is required for inner mitochondrial membrane fusion and interacts with FUNDC1 under normal conditions, contributing to mitochondrial maintenance (44). A previous study showed that OPA1 knock-down results in mitochondrial dysfunction, mitochondrial morphological changes and HF in mice (45). The present

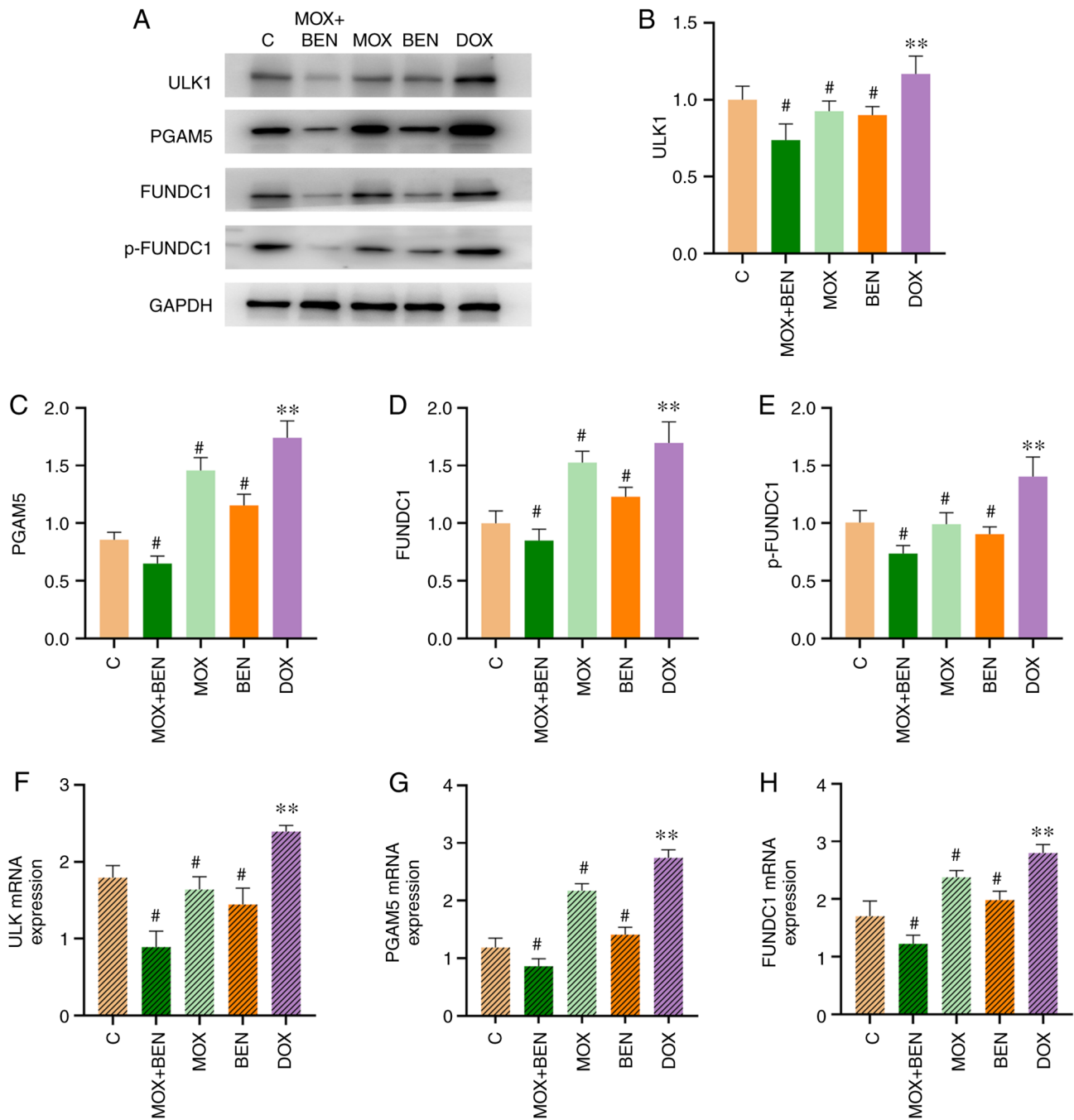


Figure 6. The effects of MOX on FUNDC1 pathway. (A) The expression levels of ULK1, PGAM5, FUNDC1, p-FUNDC1 and GAPDH. (B) ULK1 relative to GAPDH. (C) PGAM5 relative to GAPDH. (D) FUNDC1 relative to GAPDH. (E) p-FUNDC1 relative to GAPDH. (F) ULK mRNA levels. (G) PGAM5 mRNA levels. (H) FUNDC1 mRNA levels. ** $P < 0.05$ vs. C group and # $P < 0.05$ vs. DOX group. Protein levels were measured by western blotting. ULK1, PGAM5 and FUNDC1 mRNA levels were measured by RT-qPCR. Data are mean \pm standard deviation from five independent experiments ($n=13-20$). MOX moxibustion; FUNDC1, FUN14 domain-containing protein 1; ULK1, Unc-51 Like Autophagy Activating Kinase 1; PGAM5, phosphoglycerate mutase family member 5; p-, phosphorylated; DOX, doxorubicin; BEN, benazepril C, control.

study found that mitochondrial fusion was reduced in rats with CHF and increased following moxibustion treatment, an effect which may be associated with the induction of healthy mitochondrial fusion or the recycling of damaged mitochondria by mitophagy-related clearance. Mitochondrial fission is a precursor of mitophagy (43). DRP1 and FIS1 are involved in mitochondrial fission, while LC3 and p62 are the hallmark molecules of autophagy (46,47). FUNDC1 is an essential regulator of cardiac mitochondrial fission and mitophagy, recruiting DRP1 to facilitate mitochondrial fission in response to hypoxia

and directly binding with LC3 to mediate mitophagy (48). FUNDC1 regulates FIS1 at the transcriptional level by activating CREB in a Ca^{2+} -dependent manner (49). The present study indicated that DRP1, FIS1 levels and LC3II/LC3I ratio were elevated, while p62 was downregulated in the DOX group; electron microscopy also showed significantly increased number of autophagosomes, due to excessive mitochondrial fission and mitophagy under stress. Following moxibustion treatment, DRP1, FIS1 levels and LC3II/LC3I ratio as well as the amounts of autophagosomes were reduced, while p62 was

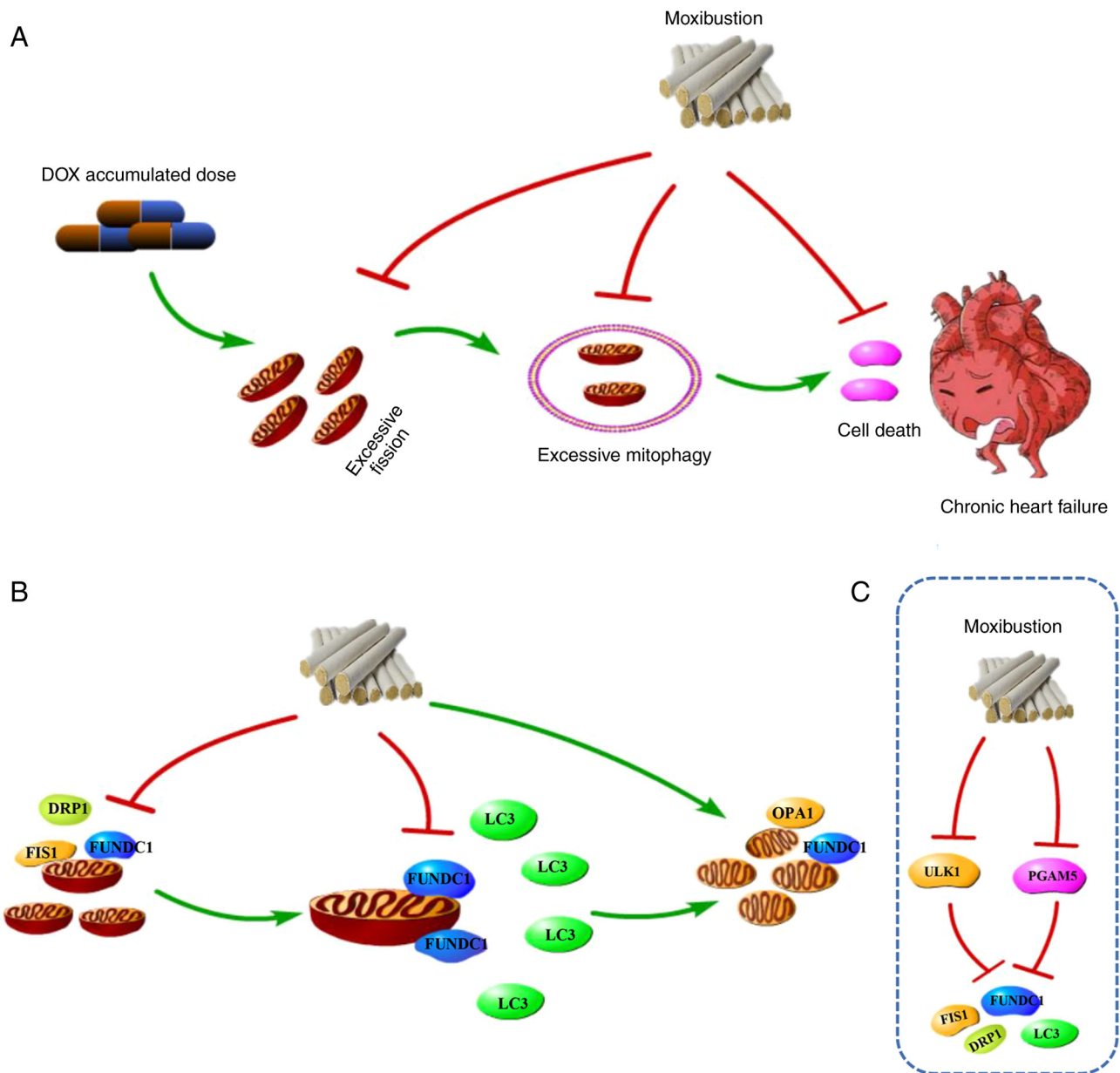


Figure 7. MOX protects the myocardium by inhibiting excessive mitochondrial fission and mitophagy through the FUNDC1 pathway. (A) DOX leads to chronic heart failure by promoting excessive mitochondrial fission and mitophagy; moxibustion could inhibit excessive mitochondrial fission and mitophagy for myocardial protection. (B) Moxibustion downregulates the mitochondrial outer membrane protein FUNDC1 and reduces the recruitment of the mitochondrial mitotic proteins DRP1, FIS1 and LC3, inhibiting excessive mitochondrial fission and mitophagy. After scavenging via mitophagy, mitochondrial fragments further occur through the binding of the mitochondrial fusion protein OPA1 to FUNDC1, resulting in mitochondrial fusion. (C) Effectors of the FUNDC1 signaling pathway. MOX moxibustion; FUNDC1, FUN14 domain-containing protein 1; DOX, doxorubicin; DRP1, dynamin-related protein 1; FIS1, fission 1 protein; OPA1, optic atrophy 1; ULK1, Unc-51 Like Autophagy Activating Kinase 1; PGAM5, phosphoglycerate mutase family member 5; DRP1, dynamin-related protein 1.

increased. These findings revealed that the protective effect of MOX on the myocardium may be related to the inhibition of excessive mitochondrial fission and mitophagy.

DOX is a non-selective class I anthracycline antibiotic, which is extensively utilized in the treatment of diverse types of cancer (50). However, its application is clinically restricted because of cumulative dose-dependent cardiotoxic effects, leading to cardiac dysfunction, cardiomyopathy, dilated cardiomyopathy and eventually CHF and mortality (51,52). A number of studies have demonstrated that DOX could produce excessive ROS in the myocardium and activate several mitochondria-related apoptotic signals, leading to myocardial

cell death (53-55). In addition, studies have reported that DOX-induced HF is associated with mitochondrial fission and autophagy (56,57). In a rat model of DOX-induced cardiomyopathy, the present study aimed to examine whether MOX inhibited mitochondrial fission and autophagy to alleviate DOX-induced HF and myocardial cell death. BEN was chosen as the positive control. A previous study found that angiotensin II (Ang II) serves a direct role in CHF development and exerts pro-autophagic effects in cardiomyocytes (58). A study demonstrated that captopril has a protective effect on prion-mediated neuronal cell death via autophagy inhibition (59).

It was previously shown that the FUNDC1 signaling pathway, a critical regulator of cardiac dynamics and mitophagy, is involved in HF (15). Therefore, regulation of mitochondrial fusion, fission and autophagy by MOX could be associated with the FUNDC1 pathway. The present study further investigated the effects of MOX on the expression levels of FUNDC1 pathway-related proteins to explore its potential protective mechanism. FUNDC1 is activated by phosphorylated/dephosphorylated ULK1 and PGAM5 to promote mitophagy, thereby controlling mitochondrial dynamics and autophagy (17) (Fig. 7). The present study showed that MOX decreased the expression levels of ULK1, PGAM5, FUNDC1 and p-FUNDC1, indicating that MOX regulates mitochondrial dynamics and mitophagy and the underlying mechanism may be related to the FUNDC1 signaling pathway. However, the FUNDC1 pathway has only been discussed initially and further FUNDC1 activators studies are needed to confirm these findings, such as the upstream protein ULK1 activator (LYN-1604 hydrochloride) or FUNDC1 gene knockout can be used for further research.

In summary, these findings confirmed that MOX improves the heart function of CHF rats by regulating mitochondrial dynamics and inhibiting autophagy. The underlying mechanism may be related to the inhibition of the FUNDC1 signaling pathway.

Acknowledgements

Not applicable.

Funding

The present study was supported by grants from the National Natural Science Foundation of China (grant no. 81574084), Key Research and Development Program of Anhui Province (grant no. 202004j07020045) and the Open Fund Project of Key Laboratory of Xin'an Medicine of the Ministry of Education (grant no. 2020xayx07).

Availability of data and materials

The datasets used and/or analyzed during the current study are available from the corresponding author on reasonable request.

Authors' contributions

JW conceived and supervised the study; JW, RX and XD designed the experiments; RX, QL and WW performed the experiments; QL, QM and BG analyzed the data; RX and JW wrote the manuscript; RX and JW performed manuscript revision. JW and RX confirm the authenticity of all the raw data. All authors reviewed the results and approved the final version of the manuscript.

Ethics approval and consent to participate

The present study was approved by the Ethics Committee of the Anhui University of Chinese Medicine [Approval No. SCXK (Shandong) 2019-003]. It was conducted on the basis of the Regulations for the Administration of Laboratory Animals in China.

Patient consent for publication

Not applicable.

Competing interests

The authors declare that they have no competing interests.

References

- Ewen S, Nikolovska A, Zivanovic I, Kindermann I and Böhm M: Chronic heart failure-new insights. *Dtsch Med Wochenschr* 141: 1560-1564, 2016 (In German).
- Tromp J, Teng TH, Tay WT, Hung CL, Narasimhan C, Shimizu W, Park SW, Liew HB, Ngarmukos T, Reyes EB, *et al*: Heart failure with preserved ejection fraction in Asia. *Eur J Heart Fail* 21: 23-36, 2019.
- Hao G, Wang X, Chen Z, Zhang L, Zhang Y, Wei B, Zheng C, Kang Y, Jiang L, Zhu Z, *et al*: Prevalence of heart failure and left ventricular dysfunction in China: The China hypertension survey, 2012-2015. *Eur J Heart Fail* 21: 1329-1337, 2019.
- van der Meer P, Gaggin HK and Dec GW: ACC/AHA versus ESC guidelines on heart failure: JACC guideline comparison. *J Am Coll Cardiol* 73: 2756-2768, 2019.
- Boorsma EM, Ter Maaten JM, Damman K, Dinh W, Gustafsson F, Goldsmith S, Burkhoff D, Zannad F, Udelson JE and Voors AA: Congestion in heart failure: A contemporary look at physiology, diagnosis and treatment. *Nat Rev Cardiol* 17: 641-655, 2020.
- Dick SA and Epelman S: Chronic heart failure and inflammation: What do we really know? *Circ Res* 119: 159-176, 2016.
- Tanai E and Frantz S: Pathophysiology of heart failure. *Compr Physiol* 6: 187-214, 2015.
- Tian R, Colucci WS, Arany Z, Bachschmid MM, Ballinger SW, Boudina S, Bruce JE, Busija DW, Dikalov S, Dorn GW II, *et al*: Unlocking the secrets of mitochondria in the cardiovascular system: Path to a cure in heart failure-a report from the 2018 national heart, lung, and blood institute workshop. *Circulation* 140: 1205-1216, 2019.
- Tahrir FG, Langford D, Amini S, Mohseni Ahooyi T and Khalili K: Mitochondrial quality control in cardiac cells: Mechanisms and role in cardiac cell injury and disease. *J Cell Physiol* 234: 8122-8133, 2019.
- Chaanine AH, LeJemtel TH and Delafontaine P: Mitochondrial pathobiology and metabolic remodeling in progression to overt systolic heart failure. *J Clin Med* 9: 3582, 2020.
- Deng Y, Xie M, Li Q, Xu X, Ou W, Zhang Y, Xiao H, Yu H, Zheng Y, Liang Y, *et al*: Targeting mitochondria-inflammation circuit by β -hydroxybutyrate mitigates HFpEF. *Circ Res* 128: 232-245, 2021.
- Muñoz JP and Zorzano A: FUNDC1: A novel protein in cardiac health. *Circulation* 136: 2267-2270, 2017.
- Meyer JN, Leuthner TC and Luz AL: Mitochondrial fusion, fission, and mitochondrial toxicity. *Toxicology* 391: 42-53, 2017.
- Chen M, Chen Z, Wang Y, Tan Z, Zhu C, Li Y, Han Z, Chen L, Gao R, Liu L and Chen Q: Mitophagy receptor FUNDC1 regulates mitochondrial dynamics and mitophagy. *Autophagy* 12: 689-702, 2016.
- Wu W, Li W, Chen H, Jiang L, Zhu R and Feng D: FUNDC1 is a novel mitochondrial-associated-membrane (MAM) protein required for hypoxia-induced mitochondrial fission and mitophagy. *Autophagy* 12: 1675-1676, 2016.
- Ma K, Zhang Z, Chang R, Cheng H, Mu C, Zhao T, Chen L, Zhang C, Luo Q, Lin J, *et al*: Dynamic PGAM5 multimers dephosphorylate BCL-xL or FUNDC1 to regulate mitochondrial and cellular fate. *Cell Death Differ* 27: 1036-1051, 2020.
- Wu W, Tian W, Hu Z, Chen G, Huang L, Li W, Zhang X, Xue P, Zhou C, Liu L, *et al*: ULK1 translocates to mitochondria and phosphorylates FUNDC1 to regulate mitophagy. *EMBO Rep* 15: 566-575, 2014.
- Jiang L, Deng Z, Zhang H, Li Y, Wang T and Xie W: Acupoint for angina pectoris: A protocol for systematic review and meta-analysis. *Medicine (Baltimore)* 100: e24080, 2021.
- Sun H, Li X, Lou J, Zhang Y, Jiang Y and Fang J: Acupuncture and related therapies for treating stable angina pectoris: A protocol of an overview of systematic reviews and meta-analysis. *Medicine (Baltimore)* 99: e23701, 2020.

20. Wang J, Zeng YL, Wu FQ, Sun RR, Chen J, Jia XZ and Xi YH: Effect of moxibustion stimulation of 'Feishu' (BL 13) and 'Xinshu' (BL 15) on expression of myocardial MyD 88 protein and caspase 3 mRNA in chronic heart failure rats. *Zhen Ci Yan Jiu* 41: 429-434, 2016 (In Chinese).
21. Liu NN, Jia XZ, Wang J, Zhu GQ, Li D, Li QL and Ma Q: Moxibustion improves cardiac function by up-regulating autophagy-related proteins of cardiomyocytes in rats with chronic heart failure. *Zhen Ci Yan Jiu* 44: 25-30, 2019 (In Chinese).
22. Li Q, Wang W, Ma Q, Xia R, Gao B, Zhu G and Wang J: Moxibustion improves chronic heart failure by inhibiting autophagy and inflammation via upregulation of mTOR expression. *Evid Based Complement Alternat Med* 2021: 6635876, 2021.
23. National Research Council (US) Committee for the Update of the Guide for the Care and Use of Laboratory Animals: Guide for the Care and Use of Laboratory Animals. 8th edition. National Academies Press (US), Washington (DC).
24. Leontyev S, Schlegel F, Spath C, Schmiedel R, Nichtitz M, Boldt A, Rübsamen R, Salameh A, Kostelka M, Mohr FW and Dhein S: Transplantation of engineered heart tissue as a biological cardiac assist device for treatment of dilated cardiomyopathy. *Eur J Heart Fail* 15: 23-35, 2013.
25. Qi Q, Liu YN, Jin XM, Zhang LS, Wang C, Bao CH, Liu HR, Wu HG and Wang XM: Moxibustion treatment modulates the gut microbiota and immune function in a dextran sulphate sodium-induced colitis rat model. *World J Gastroenterol* 24: 3130-3144, 2018.
26. Zhu Y, Zhao J, Han Q, Wang Z, Wang Z, Dong X, Li J, Liu L and Shen X: The effect and mechanism of Chinese herbal formula *sini tang* in heart failure after myocardial infarction in rats. *Evid Based Complement Alternat Med* 2018: 5629342, 2018.
27. Livak KJ and Schmittgen TD: Analysis of relative gene expression data using real-time quantitative PCR and the 2(-Delta Delta C(T)) method. *Methods* 25: 402-408, 2001.
28. Shin NR, Ryu HW, Ko JW, Park SH, Yuk HJ, Kim HJ, Kim JC, Jeong SH and Shin IS: *Artemisia argyi* attenuates airway inflammation in ovalbumin-induced asthmatic animals. *J Ethnopharmacol* 209: 108-115, 2017.
29. Shin NR, Park SH, Ko JW, Ryu HW, Jeong SH, Kim JC, Shin DH, Lee HS and Shin IS: *Artemisia argyi* attenuates airway inflammation in lipopolysaccharide induced acute lung injury model. *Lab Anim Res* 33: 209-215, 2017.
30. Lee H, Jang D, Jeon J, Cho C, Choi S, Han SJ, Oh E, Nam J, Park CH, Shin YS, *et al*: *Seomae mugwort* and *jaceosidin* attenuate osteoarthritic cartilage damage by blocking IκB degradation in mice. *J Cell Mol Med* 24: 8126-8137, 2020.
31. Ge YB, Wang ZG, Xiong Y, Huang XJ, Mei ZN and Hong ZG: Anti-inflammatory and blood stasis activities of essential oil extracted from *Artemisia argyi* leaf in animals. *J Nat Med* 70: 531-538, 2016.
32. Wang C, Yang M, Fan Y and Pei X: Moxibustion as a therapy for breast cancer-related lymphedema in female adults: A preliminary randomized controlled trial. *Integr Cancer Ther* 18: 1534735419866919, 2019.
33. Sun YJ, Yuan JM and Yang ZM: Effectiveness and safety of moxibustion for primary insomnia: A systematic review and meta-analysis. *BMC Complement Altern Med* 16: 217, 2016.
34. Ma F, Yan X, Yu Y, Du D, Li S, Chen C, Zhang X, Dong Z, Ma Y and Ma Y: Effects of herb-partitioned moxibustion for primary dysmenorrhea: A protocol for systematic review and meta-analysis. *Medicine (Baltimore)* 99: e21253, 2020.
35. Xu F, Huang M, Jin Y, Kong Q, Lei Z and Wei X: Moxibustion treatment for primary osteoporosis: A systematic review of randomized controlled trials. *PLoS One* 12: e0178688, 2017.
36. Chen L, Huang Z, Cheng K, Wu F, Deng H, Lin L, Zhao L and Shen X: The efficacy of jade moxibustion in knee osteoarthritis. *Medicine (Baltimore)* 99: e19845, 2020.
37. Stein DJ: Massage acupuncture, moxibustion, and other forms of complementary and alternative medicine in inflammatory bowel disease. *Gastroenterol Clin North Am* 46: 875-880, 2017.
38. Shin KM, Park JE, Yook TH, Kim JU, Kwon O and Choi SM: Moxibustion for prehypertension and stage I hypertension: A pilot randomized controlled trial. *Integr Med Res* 8: 1-7, 2019.
39. Yao Q, Zhang X, Huang Y, Wang H, Hui X and Zhao B: Moxibustion for treating patients with hyperlipidemia: A systematic review and meta-analysis protocol. *Medicine (Baltimore)* 98: e18209, 2019.
40. Liang B, Yan C, Zhang L, Yang Z, Wang L, Xian S and Lu L: The effect of acupuncture and moxibustion on heart function in heart failure patients: A systematic review and meta-analysis. *Evid Based Complement Alternat Med* 2019: 6074967, 2019.
41. Koch RE, Josefson CC and Hill GE: Mitochondrial function, ornamentation, and immunocompetence. *Biol Rev Camb Philos Soc* 92: 1459-1474, 2017.
42. Morales PE, Arias-Durán C, Ávalos-Guajardo Y, Aedo G, Verdejo HE, Parra V and Lavandero S: Emerging role of mitophagy in cardiovascular physiology and pathology. *Mol Aspects Med* 71: 100822, 2020.
43. Vázquez-Trincado C, García-Carvajal I, Pennanen C, Parra V, Hill JA, Rothermel BA and Lavandero S: Mitochondrial dynamics, mitophagy and cardiovascular disease. *J Physiol* 594: 509-525, 2016.
44. Wai T, Garcia-Prieto J, Baker MJ, Merkwirth C, Benit P, Rustin P, Rupérez FJ, Barbas C, Ibañez B and Langer T: Imbalanced OPA1 processing and mitochondrial fragmentation cause heart failure in mice. *Science* 350: aad0116, 2015.
45. Chen L, Gong Q, Stice JP and Knowlton AA: Mitochondrial OPA1, apoptosis, and heart failure. *Cardiovasc Res* 84: 91-99, 2009.
46. Horbay R and Bilyy R: Mitochondrial dynamics during cell cycling. *Apoptosis* 21: 1327-1335, 2016.
47. Jiang P and Mizushima N: LC3- and p62-based biochemical methods for the analysis of autophagy progression in mammalian cells. *Methods* 75: 13-18, 2015.
48. Chai P, Cheng Y, Hou C, Yin L, Zhang D, Hu Y, Chen Q, Zheng P, Teng J and Chen J: USP19 promotes hypoxia-induced mitochondrial division via FUNDC1 at ER-mitochondria contact sites. *J Cell Biol* 220: e202010006, 2021.
49. Wu S, Lu Q, Wang Q, Ding Y, Ma Z, Mao X, Huang K, Xie Z and Zou MH: Binding of FUN14 domain containing 1 with inositol 1,4,5-trisphosphate receptor in mitochondria-associated endoplasmic reticulum membranes maintains mitochondrial dynamics and function in hearts in vivo. *Circulation* 136: 2248-2266, 2017.
50. Gong J, Yan J, Forscher C and Hendifar A: Aldoxorubicin: A tumor-targeted doxorubicin conjugate for relapsed or refractory soft tissue sarcomas. *Drug Des Devel Ther* 12: 777-786, 2018.
51. Green PS and Leeuwenburgh C: Mitochondrial dysfunction is an early indicator of doxorubicin-induced apoptosis. *Biochim Biophys Acta* 1588: 94-101, 2002.
52. Koleini N and Kardami E: Autophagy and mitophagy in the context of doxorubicin-induced cardiotoxicity. *Oncotarget* 8: 46663-46680, 2017.
53. Songbo M, Lang H, Xinyong C, Bin X, Ping Z and Liang S: Oxidative stress injury in doxorubicin-induced cardiotoxicity. *Toxicol Lett* 307: 41-48, 2019.
54. Zhao L, Qi Y, Xu L, Tao X, Han X, Yin L and Peng J: MicroRNA-140-5p aggravates doxorubicin-induced cardiotoxicity by promoting myocardial oxidative stress via targeting Nrf2 and Sirt2. *Redox Biol* 15: 284-296, 2018.
55. Pan JA, Zhang H, Lin H, Gao L, Zhang HL, Zhang JF, Wang CQ and Gu J: Irisin ameliorates doxorubicin-induced cardiac perivascular fibrosis through inhibiting endothelial-to-mesenchymal transition by regulating ROS accumulation and autophagy disorder in endothelial cells. *Redox Biol* 46: 102120, 2021.
56. Catanzaro MP, Weiner A, Kaminaris A, Li C, Cai F, Zhao F, Kobayashi S, Kobayashi T, Huang Y, Sesaki H and Liang Q: Doxorubicin-induced cardiomyocyte death is mediated by unchecked mitochondrial fission and mitophagy. *FASEB J* 33: 11096-11108, 2019.
57. Mancilla TR, Davis LR and Aune GJ: Doxorubicin-induced p53 interferes with mitophagy in cardiac fibroblasts. *PLoS One* 15: e0238856, 2020.
58. Porrello ER, D'Amore A, Curl CL, Allen AM, Harrap SB, Thomas WG and Delbridge LM: Angiotensin II type 2 receptor antagonizes angiotensin II type 1 receptor-mediated cardiomyocyte autophagy. *Hypertension* 53: 1032-1040, 2009.
59. Moon JH, Jeong JK, Hong JM, Seol JW and Park SY: Inhibition of Autophagy by captopril attenuates prion peptide-mediated neuronal apoptosis via AMPK activation. *Mol Neurobiol* 56: 4192-4202, 2019.

